THE JOURNAL OF BIOLOGICAL CHEMISTRY VOL. 280, NO. 49, pp. 40813–40819, December 9, 2005

Regulation of NAD(P)H Oxidase by Associated Protein Disulfide Isomerase in Vascular Smooth Muscle Cells*

Received for publication, August 22, 2005, and in revised form, September 7, 2005 Published, JBC Papers in Press, September 8, 2005, DOI 10.1074/jbc.M509255200

Mariano Janiszewski[‡§1], Lucia Rossetti Lopes[¶1], Alípio O. Carmo[‖], Marcelo A. Pedro[‡], Ralf P. Brandes[§], Célio X. C. Santos[‡], and Francisco R. M. Laurindo[‡2]

From the [‡]Vascular Biology Laboratory, Heart Institute (Instituto do Coração), School of Medicine, University of São Paulo, Av. Eneas Carvalho Aguiar, 44-subsolo, São Paulo, CEP 05403-000 Brazil, the [§]Institut für Kardiovaskuläre Physiologie, J. W. Goethe Universität Frankfurt, D-60596 Frankfurt am Main, Germany, the [¶]Department of Pharmacology, Institute of Biomedical Sciences, University of São Paulo, São Paulo CEP 05508-900, Brazil, and the [‖]Hospital Israelita Albert Einstein, São Paulo CEP 05651-901, Brazil

NAD(P)H oxidase, the main source of reactive oxygen species in vascular cells, is known to be regulated by redox processes and thiols. However, the nature of thiol-dependent regulation has not been established. Protein disulfide isomerase (PDI) is a dithiol/disulfide oxidoreductase chaperone of the thioredoxin superfamily involved in protein processing and translocation. We postulated that PDI regulates NAD(P)H oxidase activity of rabbit aortic smooth muscle cells (VSMCs). Western blotting confirmed robust PDI expression and shift to membrane fraction after incubation with angiotensin II (AII, 100 nM, 6 h). In VSMC membrane fraction, PDI antagonism with bacitracin, scrambled RNase, or neutralizing antibody led to 26–83% inhibition ($p < 0.05$) of oxidase activity. AII incubation led to significant increase in oxidase activity, accompanied by a 6-fold increase in PDI refolding isomerase activity. AII-induced NAD(P)H oxidase activation was inhibited by 57–71% with antisense oligonucleotide against PDI (PDIasODN). Dihydroethidium fluorescence showed decreased superoxide generation due to PDIasODN. Confocal microscopy showed co-localization between PDI and the oxidase subunits $p22^{phox}$, Nox1, and Nox4. Co-immunoprecipitation assays supported spatial association between PDI and oxidase subunits $p22^{phox}$, Nox1, and Nox4 in VSMCs. Moreover, in HEK293 cells transfected with green fluorescent protein constructs for Nox1, Nox2, and Nox4, each of these subunits co-immunoprecipitated with PDI. Akt phosphorylation, a known downstream pathway of AII-driven oxidase activation, was significantly reduced by PDIasODN. These results suggest that PDI closely associates with NAD(P)H oxidase and acts as a novel redox-sensitive regulatory protein of such enzyme complex, potentially affecting subunit traffic/assembling.

Redox-dependent signal transduction, a central aspect of vascular physiology and pathophysiology, converges on enzyme systems generating reactive oxygen species, required to act as second messengers of cell stimulators such as angiotensin II (AII)[3] (1). Vascular isoforms of phagocyte NAD(P)H oxidase appear to be the most prominent source of basal as well as agonist-induced reactive oxygen species in the vessel (1–4). Yet, mechanisms that control activity of this multisubunit enzyme complex are incompletely understood. Most studies (reviewed in Refs. 3 and 4) have focused on issues related to subunit structure, undermining other aspects. We have previously shown that specific thiol oxidants/alkylators inhibit vascular NAD(P)H oxidase activity in a way that does not correlate with their induced decrease in intracellular glutathione levels (5). Moreover, recent evidence further suggests that oxidase activity is redox-regulated (4, 6, 7). These data point to the existence of yet unidentified redox-sensitive domains such as reactive thiol groups within the oxidase complex milieu. Accordingly, although thiols are key redox-signaling effectors, kinetics of spontaneous thiol-disulfide exchange, based solely on cell redox status, may be too slow to account for efficient target enzyme regulation (8–10). In turn, thiol oxidoreductases catalyze thiol reactions up to 10^4 times faster and may therefore have an important signaling role, as shown, *e.g.* for the reductase thioredoxin (8, 11). Our hypothesis is that thiol oxidoreductases act as regulators of vascular NAD(P)H oxidase. We focused into the thioredoxin superfamily enzyme protein disulfide isomerase (PDI), given its abundance, multiple biological effects, versatile redox behavior, and known interaction with other proteins (10, 12, 13). PDI is mainly located at endoplasmic reticulum (ER) lumen, where it assists in redox protein folding, which involves both oxidation and multiple intramolecular thiol-disulfide exchanges, *i.e.* isomerase, activities. Such properties stem from its structural configuration, which consists of five modules ordered as *a-b-b′-a′-c*, in which *a* is a thioredoxin domain bearing the redox-active WCGHCK motif, *b* a thioredoxin structural fold without the redox motif, possibly related to peptide recognition (12, 13), and *c* a putative Ca^{2+}-binding C-terminal domain (12, 14). Redox-active cysteines at the *a* domain exist as reduced dithiols or intramolecular or mixed disulfides. Several PDI analogues have been described, indicating that PDI is part of a larger protein family variably displaying thiol oxidoreductase, chaperone, and isomerase properties (8–10,13). Despite bearing the C-terminal ER retention sequence KDEL, PDI displays active intracellular traffic to the cell surface, where it likely acts as a reductase due to the high local reducing potential (10, 12, 13). This property led to further exploration of other cellular PDI effects. PDI-induced modification of membrane protein cysteines (15) may have roles such as cell surface recognition in cell-to-cell contact (16), shedding of L-selectin (17), chemokine receptor-dependent HIV cell internalization (18), binding and export of proteins such as thyroglobulin (19), and integrin-dependent platelet adhesion (20). In particular, PDI is a major catalyst of trans-nitrosation reactions mediating nitric oxide internalization from extracellular *S*-nitrosothiols (21, 22). In the present study, we addressed the hypothesis that PDI interacts functionally and spatially with vascular smooth muscle cell (VSMC) NAD(P)H oxidase

* This work was supported by Fundação de Amparo à Pesquisa do Estado de São Paulo, Financiadora de Estudas e Projetos/Programa de Núcleos de Excelência, F. Zerbini, the A. Einstein Society, and a Georg-Forster Grant from the Alexander von Humboldt Foundation (to M. J.). The costs of publication of this article were defrayed in part by the payment of page charges. This article must therefore be hereby marked "*advertisement*" in accordance with 18 U.S.C. Section 1734 solely to indicate this fact.

[1] Both authors contributed equally to this work.

[2] To whom correspondence should be addressed. Tel.: 55-(11)-3069-5184; Fax: 55-(11)-3069-5920; E-mail: expfrancisco@incor.usp.br.

[3] The abbreviations used are: AII, angiotensin II; DHE, dihydroethidium; PDIasODN, PDI antisense oligonucleotide; ScbRNase, scrambled RNase; ScrODN, scrambled oligonucleotide; ER, endoplasmic reticulum; VSMC, vascular smooth muscle cell; ODN, oligodeoxynucleotide; YFP, yellow fluorescent protein; GFP, green fluorescent protein; DMPO, 5,5′-dimethylpyrroline-*N*-oxide; IP, immunoprecipitation.

and that such interaction affects redox-dependent consequences of AII exposure.

MATERIALS AND METHODS

Cell Culture and Membrane Fraction Preparation—Rabbit aortic smooth muscle cells (VSMCs) from a previously established selection-immortalized line (23) were grown in Ham's F-12 medium. Membrane homogenates were prepared as described previously (24), and protein concentration was assessed by Bradford method. NADPH oxidase activity was assessed as described before (24).

Antisense Oligonucleotides—Confluent (~80%) VSMCs were transfected with PDI antisense (PDIasODN) or a scrambled control (ScrODN) oligonucleotide as described (21). Antisense (5′-GGAGC-GAGACTCCGAACAACACGGTA-3′) and ScrODNs (5′-GATG-GCACAAGCCTCAGAGCGACGG-3′) were from Sequitur, Inc. VSMCs were incubated with 20 nM ODN in SuperFect™ (reagent (Qiagen, 1:50, v/v) in fetal bovine serum-containing culture medium. Transfection dynamics was monitored with a fluorescein isothiocyanate-labeled ODN. After a 4-h incubation, cells were gently washed and maintained in F-12 medium.

Fusion Nox-GFP Constructs—Determination of a putative direct PDI interaction with Nox1 or Nox4 is complicated by their low expression levels and by lack of good specific antibodies. To ameliorate these problems, we used plasmid constructs coding for fusion proteins of Nox subunits with yellow fluorescent protein (YFP), a variant of green fluorescent protein, transiently transfected into HEK 293 cells (American Type Culture Collection). This strategy allows direct observation of tagged proteins and their detection through anti-GFP antibody (from Roche Applied Science). Details of this procedure and several validation experiments were described previously (25). Briefly, plasmids coding for full-length Nox1, Nox4, or Nox2 were tagged with YFP at the C-terminal end and transfected into HEK293 cells (10 μg of plasmid DNA for 10-cm culture dishes at ~90% confluence) using Lipofectamine™ 2000 according to the manufacturer's instructions (Invitrogen). Experiments were performed 24 h after transfection.

PDI Inhibitors—Known PDI inhibitors used in our study at previously validated concentrations were bacitracin (500 μM), scbRNase (RNase with scrambled disulfide bonds, 100 μg/ml, from Sigma), a competitive substrate, or the neutralizing monoclonal PDI antibody RL90 (1:100, Affinity Bioreagents) (26–28). The thiol reagent dithionitrobenzoic acid (500 μM), which has been reported to inhibit both NADPH oxidase (5) and PDI (18) activities, was also used. Inhibitors were added to the assay 15 min prior to measurements.

EPR Experiments—EPR experiments were performed as described (5, 24, 29) using 20 μg of VSMC membrane fraction protein incubated for 10 min at 37 °C with the spin trap 5,5′-dimethylpyrroline-*N*-oxide (DMPO, 50 mM) in 1 ml of phosphate-buffered saline with 10 μM DTPA, pH 7.4. Enzyme activity was started by 300 μM NAD(P)H in the absence or presence of PDI inhibitors. Incubation medium was then transferred to a flat quartz cell, and spectra were cumulatively recorded (8 scans) at room temperature using a Bruker EMX 300 spectrometer with conditions: microwave power, 40 milliwatts; modulation amplitude, 1.0 G; time constant, 200 ms; scan rate, 0.1 G/s; gain, 3.2×10^6. DMPO-OH spin adduct was quantified assessing the central peak height as a linear function of a standard (38 μM) concentration of 4-hydroxy-2,2,6,6-tetramethyl-1-piperidinyloxy (Tempol).

Superoxide Measurement in Intact VSMCs—Confluent (~80%) VSMCs grown on glass slides were transfected with PDIasODN or ScrODN as described above. Control or AII-stimulated cells (100 nM for 6 h) were incubated with dihydroethidium (DHE, 5 μM) for 30 min at room temperature and imaged by fluorescence microscopy (Axiovert 200, Zeiss), with exposure intensity adjusted relative to baseline VSMCs (30).

RNase Refolding Analysis—Disulfide isomerase activity was assessed in VSMCs membrane fraction through the ability to reconstitute the RNase activity of scbRNase (31, 32). RNA hydrolysis rate was monitored spectrophotometrically (GeneQuantPro™) at 260 nm. Bovine liver PDI (Sigma) was used as positive control.

Confocal Microscopy—Confluent (~70%) VSMCs were grown on collagen-coated glass slides, transfected or not with PDIasODN or ScrODNs as described above, and incubated in the absence or presence of AII (100 nM, 12 h). Forty-eight hours after transfection, cells were fixed in phosphate-buffered paraformaldehyde solution (4%), washed in phosphate-buffered saline, blocked for 1 h with 5% bovine serum albumin/phosphate-buffered saline, and incubated overnight with antibody against PDI (1:250, Affinity Bioreagents), $p22^{phox}$ (1:100, Santa Cruz Biotechnology, Santa Cruz, CA), Nox4 (1:100, Santa Cruz Biotechnology), or Nox1 (1:100, Santa Cruz Biotechnology). Immunodetection was performed with Alexa Fluor (1:250, Invitrogen)-, Rhodamine-, or fluorescein isothiocyanate (1:250, Santa Cruz Biotechnology)-conjugated secondary antibodies and co-localization studies were carried out using a Zeiss laser-scanning confocal microscope LSM 510 META in multitracking mode.

Immunoprecipitation and Western Analysis—Cells were lysed in Nonidet lysis buffer containing Tris/HCl (pH 7.4, 20 mM), NaCl (150 mM), $Na_4P_2O_7$ (10 mM), okadaic acid (10 nM), Na_3VO_4 (2 mM), leupeptin (2 μg/ml), pepstatin (2 μg/ml), trypsin inhibitor (10 μg/ml), phenylmethylsulfonyl fluoride (44 μg/ml), and Nonidet, P40 (1% v/v), left on ice for 10 min, and then centrifuged at 10,000g/10 min. Protein concentration was adjusted to 1 μg/μl, and immunoprecipitation (IP) was carried out by using 500 μg of homogenate protein. Following preclearing with protein A/G-Sepharose (Amersham Biosciences), in the absence or presence of nonspecific IgG, proteins were precipitated using an anti-PDI antibody (1.2 μg, for VSMCs, mouse monoclonal from Affinity Bioreagents RL90; for HEK293 cells, rabbit polyclonal, Stressgen). Preclearings and post-IP supernatants were loaded on separate gels to confirm specificity of the bands in the immunoprecipitation and to ascertain identical amounts of protein in the IP. Immunoprecipitates were heated (95 °C, 10 min), run on SDS-polyacrylamide gels, and then blotted onto nitrocellulose. Proteins were detected with following antibodies: Nox1 (Santa Cruz Biotechnology), Nox4 (rabbit polyclonal antibody 4014, kindly provided by Prof. Dr. J. Pfeilschifter, Klinikum der J. W. Goethe Universität, Frankfurt), and $p22^{phox}$ (mouse monoclonal antibody 449, kindly provided by Dr. D. Roos, Sanquin Research at CLB, Amsterdam University). Blots were revealed by chemiluminescence.

Akt Phosphorylation—VSMCs (~80% confluence) transfected with PDIasODN or ScrODNs as described were maintained in fetal bovine serum-containing medium for 12 h, made quiescent by further incubation in F-12 medium with 0.1% calf serum for 12 h, and then stimulated with AII at 37 °C in serum-free F-12 for 2–30 min (33). VSMCs were trypsin-lysed in 100 mM Tris buffer (pH 7.5) containing protease and phosphatase inhibitors. The homogenate was resolved by 10% SDS-PAGE, and Akt phosphorylation was assessed with monoclonal phospho-Akt (Ser-473) or total Akt antibodies (Cell Signaling Technology, 1:1000). Densitometry was performed with Scion Image Program.

Statistical Analysis—Data are mean ± S.E. Comparisons among groups were performed by one-way analysis of variance plus Student-Newman-Keuls test, at 0.05 significance level.

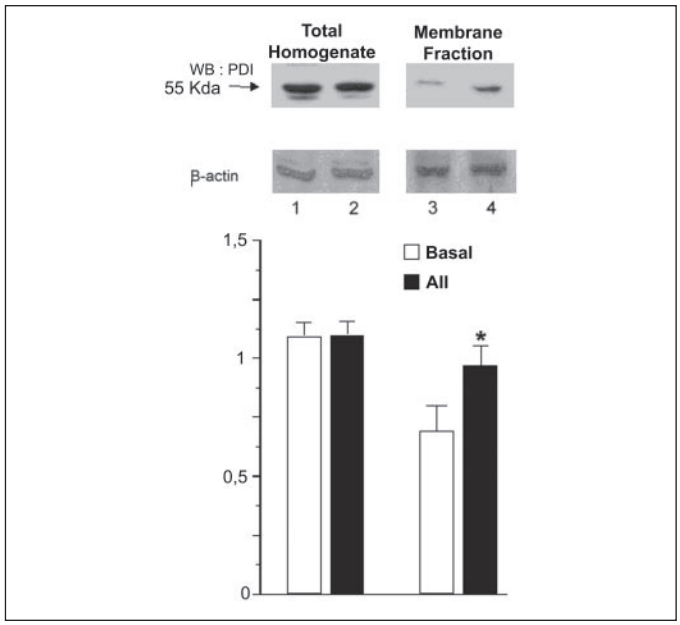

FIGURE 1. **Western blot analysis of PDI (~55 kDa) in VSMCs homogenates before and after AII incubation (100 nM, 6 h).** AII incubation had no effect in total cell PDI expression (*lane 2 versus lane 1*) while inducing clear increase in the membrane PDI pool (*lane 4 versus lane 3*), indicating PDI shift to membrane structures ($n = 4$; *, $p < 0.01$ *versus* basal condition, results normalized to β-actin expression). Data were also normalized for relevant Coomassie Blue bands (not shown), with identical results.

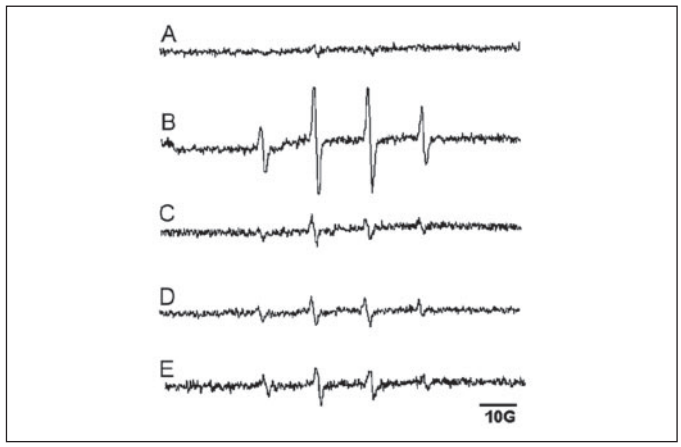

FIGURE 2. **Effect of PDI inhibitors on NADPH-driven DMPO-OH radical adduct EPR spectra in VSMCs membrane fraction.** *A*, membrane fraction preincubated with DMPO; *B*, same as in *A*, plus NADPH; *C*, same as *B*, plus 500 units/ml (polyethylene glycol) superoxide dismutase; *D*, same as in *B*, plus 500 μM bacitracin; *E*, same as in *B*, plus inhibitory anti-PDI antibody (1:100). Spectra represent 3–8 replicates of 3 independent experiments. Quantitation yields (arbitrary units *versus* standard) were as follows: *A*, undetectable; *B*, 13.9 ± 1.5; *C*, 5.2 ± 1.6 (*); *D*, 2.4 ± 1.2 (*); *E*, 6.9 ± 2.0 (*); *, $p < 0.05$ *versus B*.

RESULTS

PDI Expression in VSMCs—Western blotting analysis showed robust PDI expression in VSMCs visualized as a 55-kDda band. VSMC incubation with AII (100 nM, 6 h) did not alter total PDI expression. However, AII led to a significant shift in PDI location toward the membrane fraction (Fig. 1).

PDI Inhibition in VSMCs Membrane Fraction Decreases NAD(P)H Oxidase Activity—To assess functional dependence of NAD(P)H oxidase activity on PDI, NADPH-driven superoxide generation was assessed by EPR spectroscopy in VSMC membrane fraction incubated after its separation with known PDI inhibitors (Fig. 2). Membrane fraction alone produced no detectable signals. With NADPH, there was formation of the typical 1:2:2:1 DMPO-OH signal with splitting constants aN = 1.49 mT and aH = 1.49 mT. Adduct yields were inhibited with (polyethylene glycol) superoxide dismutase by 63%. Superoxide levels were estimated as 125.0 ± 16.8 nmol/mg of protein (34). Importantly, NADPH oxidase activity was significantly dependent on PDI, as shown by 51–83% decrease in adduct signals after homogenate incubation with bacitracin, a pharmacological antagonist of PDI oxidoreductase activity (26–28), and neutralizing anti-PDI antibody (Fig. 2), toward respective superoxide estimates of 21.6 ± 17.2 and 61.3 ± 19.0 nmol/mg. Control experiments with nonspecific anti-Histone antibody (1:100) showed no effect (not shown). Identical results were obtained using NADH as substrate (not shown).

Experiments were also performed with lucigenin chemiluminescence technique (24), showing analogous inhibition (ranging from 26 to 69%, data not shown) of NADPH oxidase activity, both at baseline or after 6-h incubation with AII, by the following PDI inhibitors, added to VSMC membrane fraction: bacitracin, anti-PDI antibody, ScbRNase, or the thiol reagent dithionitrobenzoic acid.

Because inhibition of PDI isomerase activity due to such agents is known to involve PDI thiols (18, 26–28), and all compounds were effective when incubated with membrane fraction after its separation, these results suggest that PDI co-fractionates with NAD(P)H oxidase and contributes to sustain its activity via thiol redox mechanisms.

PDI Antisense Decreases NAD(P)H Oxidase Activity and Superoxide Production in VSMCs—To further assess PDI functional interaction with NAD(P)H oxidase, we transfected VSMCs with a PDIasODN. Transfection efficiency was confirmed by average 32% decrease in PDI protein expression at Western analysis (not shown), diminished PDI RNase refolding activity (Fig. 4) and lower PDI fluorescent immunodetection (Fig. 5). Marked cellular effects due to similar rates of PDI protein decrease with antisense ODNs were reported previously (15). PDIasODN did not decrease $p22^{phox}$ expression (Fig. 5).

ScrODN induced no change in NADPH-driven signals assessed in VSMCs membrane fraction, at baseline and following 6-h incubation with AII. In contrast, PDIasODN markedly impaired oxidase activity in the same conditions by an average 71% both at baseline and after AII (Fig. 3*A*). Accordingly, as seen in Fig. 3*B*, DHE-derived fluorescent signals were increased by AII in control VSMCs or after ScrODN transfection. Such increase was completely inhibited by (polyethylene glycol) superoxide dismutase (25 units/ml, not shown). PDIasODN transfection markedly inhibited AII-induced superoxide production in VSMCs.

Increase in PDI Activity Concomitant to AII-induced NAD(P)H Oxidase Activation—To assess whether oxidase activation and PDI shift to membrane fraction induced by AII were accompanied by concomitant increase in PDI function, the refolding activity of PDI was measured (31, 32). Incubation of VSMCs with AII (100 nM for 6 h) led to marked 5-fold increase in membrane fraction-induced refolding rates of ScbRNase (Fig. 4). PDIasODN but not ScrODN transfection decreased PDI activity at baseline and particularly after AII. There was analogous inhibition with bacitracin (Fig. 4). These data further suggest that thiols are involved in PDI interaction with NAD(P)H oxidase.

Co-localization between PDI and NAD(P)H Oxidase Subunits—To assess co-localization between PDI and NAD(P)H oxidase, studies were performed first with antibodies against $p22^{phox}$ and PDI. Both at rest and following AII incubation (12 h), there was co-localization between the two proteins. At rest, both proteins co-localized at a slightly predominant perinuclear distribution (Fig. 5, *A* and *B*). PDIasODN transfection did not visibly change $p22^{phox}$, but decreased PDI signal and their co-localization at baseline (Fig. 5*C*) and after AII (Fig. 5*D*). VSMCs transfected with ScrODN were similar to non-transfected cells (Fig. 5*E*).

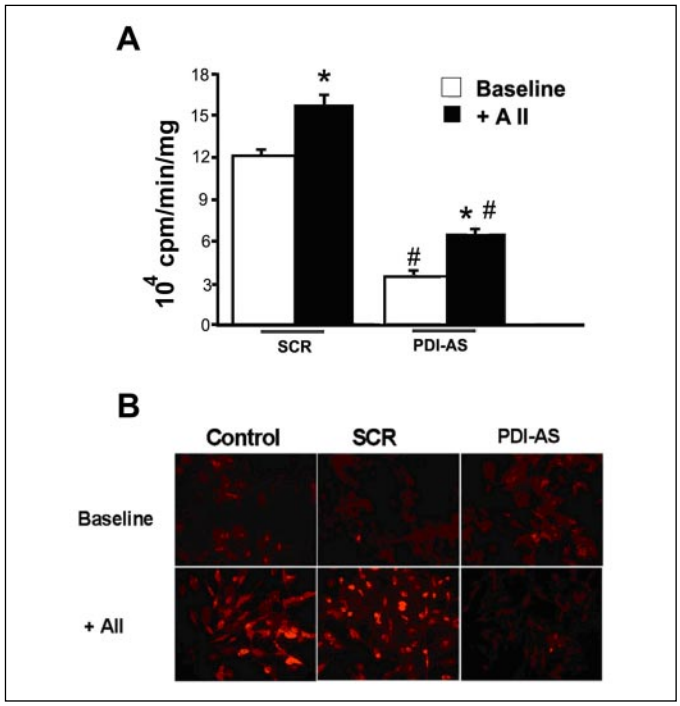

FIGURE 3. *A*, inhibitory effects of PDIasODN transfection in baseline or AII-stimulated NAD(P)H oxidase activity measured by lucigenin chemiluminescence ($n = 4$; *, $p < 0.05$ *versus* baseline; #, $p < 0.05$ *versus* ScrODN-transfected VSMCs). *B*, superoxide production in VSMCs assessed by DHE fluorescence in control VSMCs and after Scr or PDIasODN transfection, both at baseline (*upper panels*) and after AII (*lower panels*).

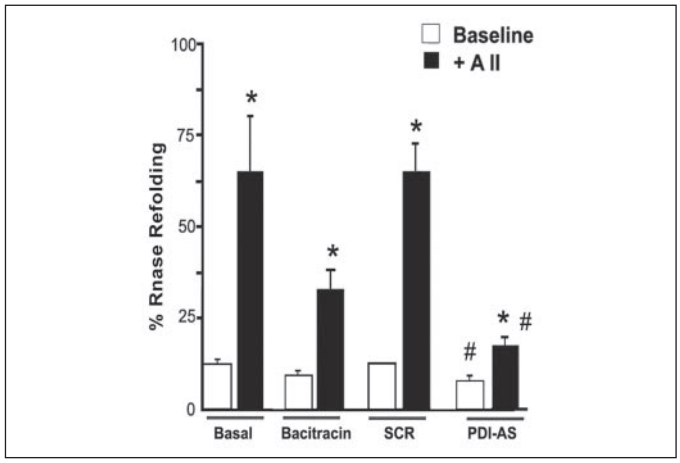

FIGURE 4. **Marked increase in PDI refolding isomerase activity in VSMCs membrane fraction after exposure to AII.** Absorbance decay at basal level was $1.00 \pm 0.13 \times 10^{-3}$ units/min^{-1}. Baseline and particularly AII-stimulated PDI activity were inhibited by bacitracin or PDIasODN, but not ScrODN. VSMCs were preincubated with Scr or PDIasODN (see "Materials and Methods") and then stimulated with AII for 6 h ($n = 6$; *, $p < 0.05$ *versus* respective baseline; #, $p < 0.05$ *versus* ScrODN-transfected VSMCs).

Further immunofluorescence studies were performed with analogous technique to investigate co-localization between PDI and the subunits Nox1 and Nox4, which, contrarily to Nox2, are the major Nox subunits expressed in VSMCs (2, 3). Our data (Fig. 6) disclosed a co-localization pattern with PDI.

Association between PDI and NAD(P)H Oxidase Subunits—The above functional and co-localization data suggested that PDI co-fractionates with NAD(P)H oxidase. Such association was further investigated by co-immunoprecipitation experiments. In VSMCs, PDI immunoprecipitation yielded co-precipitation of NAD(P)H oxidase subunits $p22^{phox}$, Nox1, and Nox 4 (Fig. 7). We further tested such results in

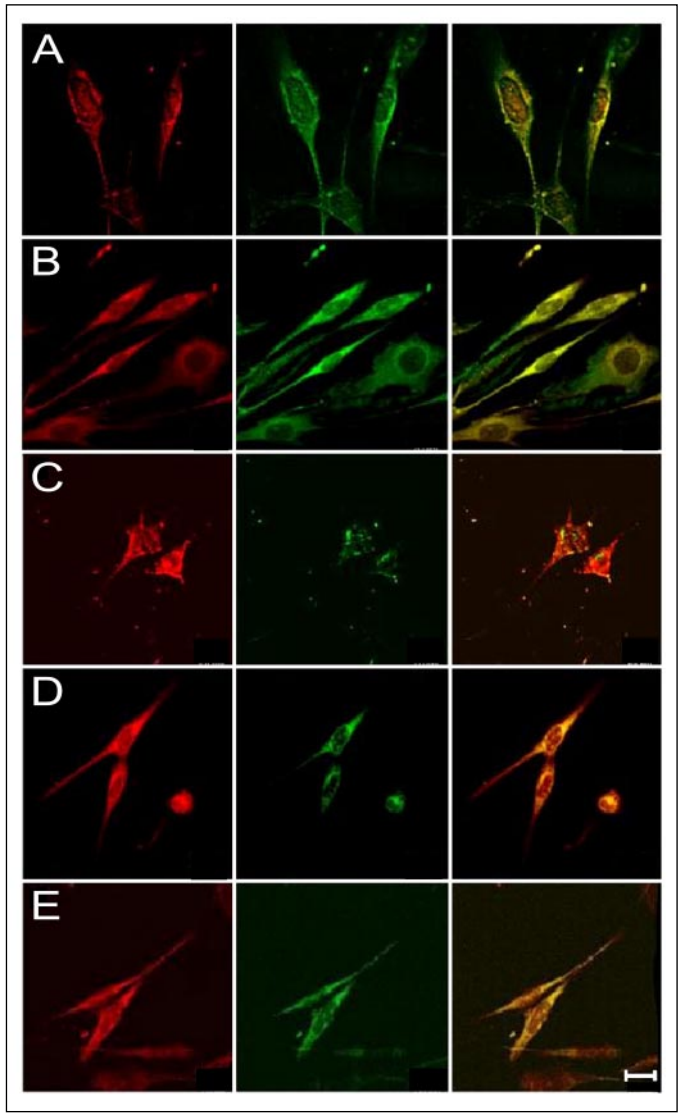

FIGURE 5. **Representative confocal laser scanning microscopy images of VSMCs incubated in the absence (*A*, *C*, and *E*) or presence (*B* and *D*) of 100 nM AII for 12 h.** PDI (*green* fluorescein isothiocyanate staining), $p22^{phox}$ (*red* TRITC staining), and co-localization of PDI and $p22^{phox}$ proteins (*yellow* staining, *right panels*) were developed as described under "Materials and Methods." Images were obtained in control VSMCs (*A* and *B*) or after transfection with PDIasODN (*C* and *D*) or ScrODN (*E*). *Magnification bar* is 20 μm.

HEK293 cells transfected with Nox-yfp coding plasmids. Precipitation of PDI revealed co-precipitation of all three Nox-yfp constructs, as observed by a band detected at the expected height by anti-GFP antibodies (Fig. 8). Both patterns of fluorescence co-localization (Fig. 5) and co-immunoprecipitation (not shown) exhibited no visible difference after VSMCs incubation with AII.

PDI Affects Akt Phosphorylation—To investigate whether interaction of PDI with NAD(P)H oxidase affects downstream oxidase signaling pathways, we determined the effect of PDI inhibition on AII-induced Akt phosphorylation, known to be dependent on NAD(P)H oxidase (2, 33) as well as reactive thiols (35). Indeed, AII-mediated Akt phosphorylation was reduced by PDIasODN, but not ScrODN (Fig. 9).

DISCUSSION

The present study provides for the first time evidence that PDI, a dithiol-disulfide oxidoreductase chaperone of the ER, acts as a regulator of VSMCs NAD(P)H oxidase and associates with its subunits. Our con-

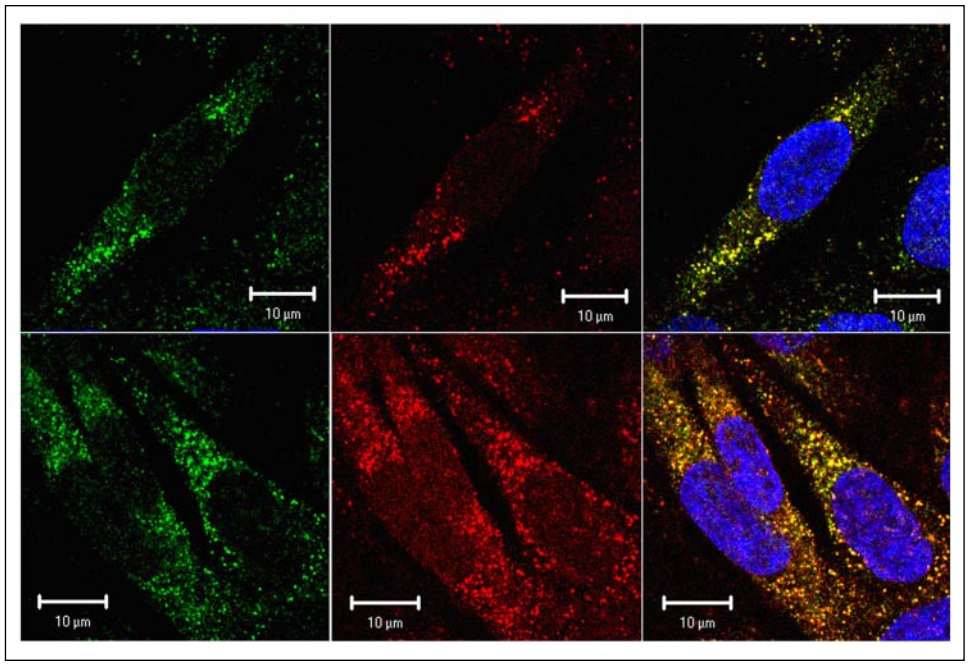

FIGURE 6. **Representative confocal microscopy images of VSMCs.** PDI is represented by the *green* staining (Alexa Fluor 488-conjugated secondary antibody) in the *left panels*, Nox1 (*upper panels*) or Nox4 (*lower panels*) are depicted as *red* (Alexa Fluor 546-conjugated secondary antibody) staining, and co-localization is shown in the *right panels* in *yellow*. *Magnification bar* is 10 μm.

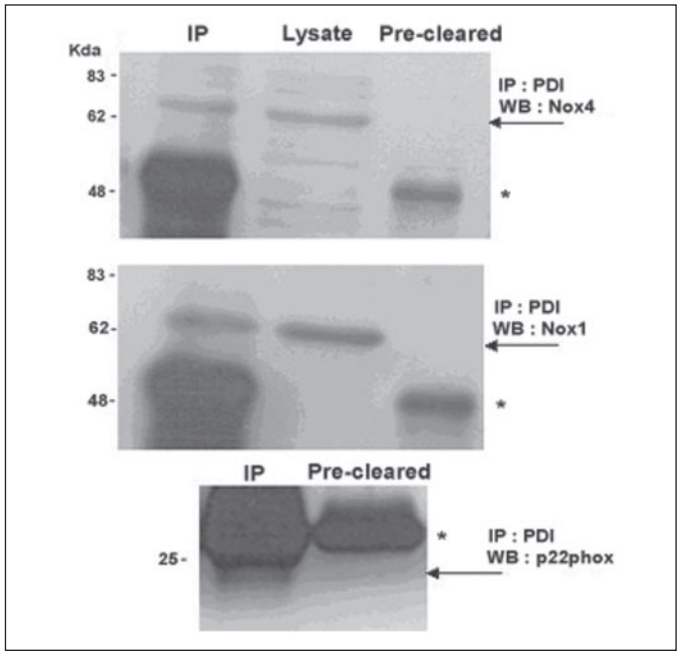

FIGURE 7. **Co-immunoprecipitation between PDI and Nox subunits in VSMCs.** Extracts from VSMCs were subjected to immunoprecipitation (*IP*) using anti-PDI antibody. Western blotting (*WB*) analysis was performed using the indicated antibodies in the IP fraction, whole cell lysate or precleared fraction, which, in this example, was obtained after sample incubation with beads and nonspecific IgG. Blots are representative of three or more similar experiments. *Asterisks* indicate nonspecific staining from heavy or light chains of IgG used for immunoprecipitation. *Arrows* indicate signals corresponding to Nox4, Nox1, and $p22^{phox}$.

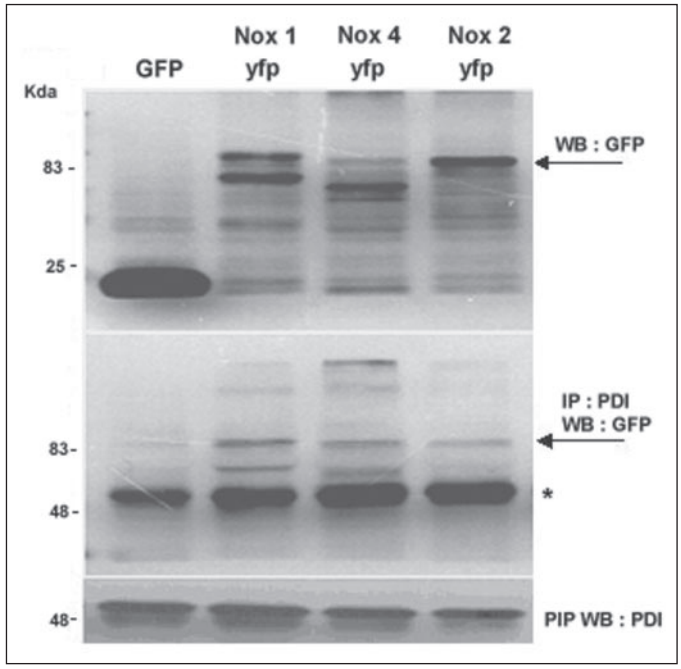

FIGURE 8. **Co-immunoprecipitation between PDI and Nox subunits in HEK293 cells transfected with Nox-yfp constructs and detected through GFP antibody (see text for details).** In the *upper panel*, Western blotting (*WB*) analysis with anti-GFP antibody of total cell extracts shows protein expression. Extracts were subjected to immunoprecipitation (*IP*) using anti-PDI antibody and revealed with Western blotting analysis using anti-GFP antibody, shown in the *middle panel*. Post-IP supernatants (*PIP*) were loaded onto separate gels and stained for PDI to document similar amounts of proteins used during the IP. Precleared controls similar to those of Fig. 7 were performed (not shown). The immunoprecipitates did not stain for yfp band (visualized with different exposure times). Blots are representative of three identical experiments. The *asterisk* indicates nonspecific staining from heavy chain of IgG used for immunoprecipitation. *Arrows* indicate signals of Nox-yfp constructs.

clusions are supported by the uniform decrease in oxidase activity or superoxide production induced by diverse strategies for antagonism of PDI function or expression. In particular, PDIasODN transfection markedly inhibited not only NAD(P)H oxidase activation and superoxide release due to AII, but also phosphorylation of Akt, a known downstream pathway of AII-induced oxidase activation, thus indicating physiological relevance for PDI-oxidase interaction. AII-induced oxidase activation was associated with a shift of PDI to membrane fraction along with increase in its isomerase activity. Co-localization and/or co-immunoprecipitation studies in VSMCs or in HEK293 cells transfected with Nox-GFP constructs supported close association between PDI and at least oxidase subunits $p22^{phox}$, Nox1, and Nox4. Thus, our results open new perspectives to clarify the intricate functional regulation of NAD(P)H oxidase.

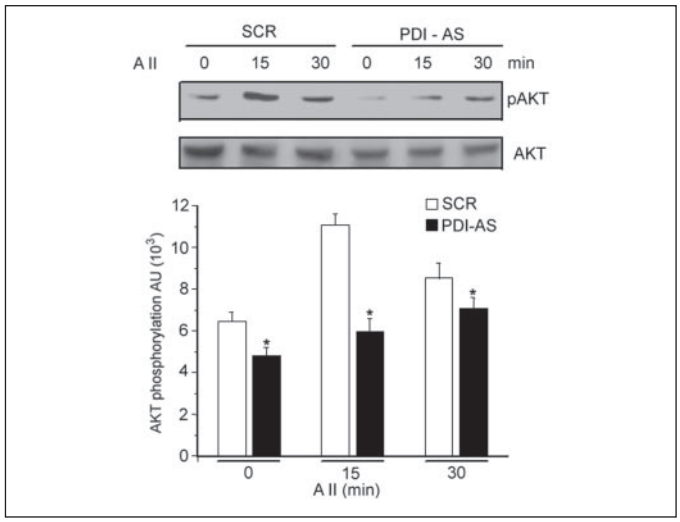

FIGURE 9. **Western blotting analysis depicting Akt phosphorylation in VSMCs at baseline or after incubation with AII for the indicated time periods.** Homogenate samples from *upper panels* were hybridized with anti-phospho-Akt, and those from *lower panels* with total Akt antibodies. VSMCs were transfected with ScrODN (*lanes 1–3*) or PDIasODN (*lanes 3–6*). The *bar graph* depicts densitometric analysis of phospho-Akt normalized to total Akt signals of three similar experiments, showing the inhibitory effect of PDIasODN on Akt phosphorylation (*, $p < 0.005$ *versus* controls).

Despite PDI abundance, its impact on overall cellular redox status does not match the more efficient and less compartmentalized glutathione or NADPH redox pairs (36). Thus, it is unlikely that PDI-oxidase interaction is mediated by changes in overall cellular redox status. In fact, our prior work clearly showed that intracellular glutathione oxidation is not sufficient for vascular oxidase inhibition (5). PDI interference with NADPH availability is also unlikely, because the latter is not a suitable PDI substrate, and our results were obtained in homogenates incubated with excess NADPH. Therefore, consistent with our data, PDI most likely exerts its regulatory effects through association with oxidase subunit(s) governing its basal or stimulated activity. The precise nature of such interaction requires further study. The observed association of PDI with diverse oxidase subunits indicates either direct binding to each Nox, binding to a common regulatory subunit (*e.g.* $p22^{phox}$), or to a regulatory domain, *e.g.* kinase/phosphatase.

Our data extend our previous observations that thiols affect NAD(P)H oxidase activity (5), suggesting in this process a potential regulatory role for dithiols, preferential PDI substrates. Because PDI redox is modulated by ambient redox potential, PDI tends to act as a reductase outside of ER (10, 12, 13, 18). However, exposure to oxidants, which can occur in specific microenvironments (37), could promote PDI thiol oxidation, which is preferentially intra- rather than intermolecular, converting PDI into a thiol oxidase/isomerase (12). Of note, although the PDI oxidase activity requires only cysteines from the *a* or *a′* domains, its reductase and in most cases isomerase activity require the entire multidomain PDI structure (38). With respect to NAD(P)H oxidase, typical thioredoxin motifs are absent among known VSMC oxidase subunits, because a detailed search of the NCBI data base yielded no hits. Still, reactive cysteines have been described for Nox2 as the dithiol binding site of phenylarsine oxide (39), and for $p47^{phox}$ (40).

On the other hand, PDI binding to other proteins in general may not occur via thiol groups (10, 12, 13, 41, 42). This seems to be the case even for other PDI family proteins, because PDI thiols are oxidized by ERO1p in the ER (12), but binding to Erp57 does not involve PDI thioredoxin domain (43). In fact, peptide binding to PDI preferentially occurs close to its C-terminal domain as a hydrophobic interaction, even though thiols contribute to subsequent binding stabilization (42). This type of interaction is involved in PDI chaperone activity, which does not require thioredoxin domains (12). Therefore, regarding PDI effects, thiol redox activity and binding to other proteins, while potentially related, are likely to be distinct processes.

Overall, such a versatility of PDI molecular interactions and redox activity underlies multiplicity of known PDI effects (10, 12, 13) and may account for diverse pathways whereby PDI may affect NAD(P)H oxidase, some of them deserving further discussion. First, as a redox chaperone (12), PDI binding to oxidase subunits may help stabilize their intra- or intermolecular configuration. In addition, the low pK_a of the exposed N-terminal cysteine of WCGHCK domain (10, 12) renders PDI a preferential target of hydrogen peroxide-mediated oxidation (44) or glutathiolation (45). Such a sensitivity may provide PDI with a role as mediator of redox regulation of NAD(P)H oxidase. Increasing evidence for this mode of regulation includes the known stimulation of oxidase activity by exogenous hydrogen peroxide (4, 7), as well as the biphasic nature of vascular cell NAD(P)H oxidase activation due to AII (46), growth factors (4), or thrombin (4, 6). In this model, a transient early agonist-triggered peak of hydrogen peroxide seems essential to sustain oxidase activation, in connection with increased subunit expression (6). On the other hand, while exposure to low hydroperoxide concentrations also stimulates oxidase activity in alveolar macrophages, higher but non-lethal concentrations inhibit the respiratory burst (47). Our finding that PDI clearly associates with oxidase subunits in unstimulated VSMCs is in line with the reported preassembling of $p22^{phox}$ and Nox1/Nox4 in resting cells (3, 4, 25). Of note, although our results focused on oxidase regulation by PDI, the potentially complex *in vivo* hierarchy of such protein interactions leave open the possibility that NAD(P)H oxidase also regulates some yet undisclosed PDI functions.

Finally, an important context in which PDI may exert its regulatory effects is protein processing and/or traffic among ER, cell membranes, and extracellular milieu (48). Indeed, it is known that PDI migrates distally from the ER enough to affect the redox state of cell-surface (15, 21, 22) or adhesion molecule (20) thiols. Thus, association with PDI potentially influences cellular traffic or assembling of oxidase subunits and underscores the secretory pathway as a likely scenario for oxidase activation. Indeed, it is known that oxidase activation in endothelial (49) or smooth muscle cells (50) is simultaneous to shift of subunit(s) from perinuclear region to membranes. The phagocyte oxidase also displays active subcellular traffic (51), in line with the recent description of JFC, a 62-kDa subunit that binds to $p67^{phox}$ and phosphoinositides, involved in vesicle translocation to plasma membrane (52).

Interestingly, recent work described the novel thioredoxin superfamily PDI-homologue EFP1 and its close association with Duoxs proteins of the Nox family as partner of enzyme complex assembly at the plasma membrane (53).

In summary, our data indicate that PDI acts as a novel regulatory protein of VSMCs NAD(P)H oxidase. Overall, PDI thiol redox properties and its role in intracellular protein traffic suggest a link with redox-regulated mechanisms associated with compartmentalization and fine-tuning of reactive oxygen species production. Further elucidation of such mechanisms may have considerable implications regarding a novel model of oxidase regulation and allowing design of more precise therapeutic interventions.

Acknowledgments—We are grateful for the help of Prof. Kleber Franchini (Unicamp) with confocal images and Prof. Ohara Augusto (Instituto de Química da Universidade de São Paulo) with EPR assays.

REFERENCES

1. Finkel, T. (2003) *Curr. Opin. Cell Biol.* **15,** 247–254
2. Griendling, K. K., Sorescu, D., and Ushio-Fukai, M. (2000) *Circ. Res.* **86,** 494–501
3. Lassègue, B., and Clempus, R. E. (2003) *Am. J. Physiol.* **285,** R277–R297
4. Brandes, R. P., and Kreuzer, J. (2005) *Cardiovasc. Res.* **65,** 16–27
5. Janiszewski, M., Pedro, M. A., Scheffer, R. C. H., van Asseldonk, J.-T. H., Souza, L. C., da Luz, P. L., Augusto, O., and Laurindo, F. R. M. (2000) *Free Radic. Biol. Med.* **29,** 889–899
6. Djordevic, T., Pogrebniak, A., BelAiba, R. S., Bonello, S., Wotzlaw, C., Acker, H., Hess, J. and Gorlach, A. (2005) *Free Radic. Biol. Med.* **38,** 616–630
7. Colston, J. T., Rosa, S. D., Strader, J. R., Anderson, M. A., and Freeman, G. L. (2005) *FEBS Lett.* **579,** 2533–2540
8. Arrigo, A.-P. (1999) *Free Radic. Biol. Med.* **27,** 936–944
9. Frand, A. R., Cuozzo, J. W., and Kaiser, C. A. (2000) *Trends Cell Biol.* **10,** 203–210
10. Noiva, R. (1999) *Semin. Cell Dev. Biol.* **10,** 481–493
11. Yamawaki, H., Haendeler, J., and Berk, B. (2003) *Circ. Res.* **93,** 1029–1033
12. Wilkinson, B., and Gilbert, H. F. (2004) *Biochim. Biophys. Acta* **1699,** 35–44
13. Clissold, P. M., and Bicknell, R. (2003) *BioEssays* **25,** 603–611
14. Freedman, R. B., Hirst, T. R., and Tuite, M. F. (1994) *Trends Biochem. Sci.* **19,** 331–336
15. Jiang, X. M., Fitzgerald, M., Grant, C. M., and Hogg, P. J. (1999) *J. Biol. Chem.* **274,** 2416–2423
16. Rao, A. S. M. K., and Hausman, R. E. (1993) *Proc. Natl. Acad. Sci. U. S. A.* **90,** 2950–2954
17. Bennett, T. A., Edwards, B. S., Sklar, L. A., and Rogely, S. (2000) *J. Immunol.* **164,** 4120–4129
18. Gallina, A., Hanley, T. M., Mandel, R., Trahey, M., Broder, C. C., Viglianti, G. A., and Ryser, H. J.-P. (2002) *J. Biol. Chem.* **277,** 50579–50588
19. Delom, F., Mallet, B., Carayon, P., and Lejeune, P. J. (2001) *J. Biol. Chem.* **276,** 21337–21342
20. Lahav, J., Wijnem, E. M., Hess, O., Hamaia, S. W., Griffiths, D., Makris, M., Knight, G., Essex, D. W., and Farndale, R. W. (2003) *Blood* **102,** 2085–2092
21. Zai, A., Rudd, M. A., Scribner, A. W., and Loscalzo, J. (1999) *J. Clin. Invest.* **103,** 393–399
22. Ramachandran, N., Root, P., Jiang, X.-M., Hogg, P. J., and Mutus, B. (2001) *Proc. Natl. Acad. Sci. U. S. A.* **98,** 9539–9544
23. Buonassissi, V., Venter, J. C. (1976) *Proc. Natl. Acad. Sci. U. S. A.* **73,** 1612–1616
24. Laurindo, F. R. M., Souza, H. P., Pedro, M. P., and Janiszewski, M. (2002) *Methods Enzymol.* **352,** 432–454
25. Ambasta, R. K., Kumar, P., Griendling, K. K., Schmidt, H. H., Busse, R., and Brandes, R. P. (2004) *J. Biol. Chem.* **279,** 45935–45941
26. Orlandi, P. A. (1997) *J. Biol. Chem.* **272,** 4591–4599
27. Mandel, R., Ryser, H. J., Ghani, F., Wu, M., and Peak, D. (1993) *Proc. Natl. Acad. Sci. U. S. A.* **90,** 4112–4116
28. Essex, D. W., and Li, M. (1999) *Br. J. Haematol.* **104,** 448–456
29. Janiszewski, M., Souza, H. P., Liu, X., Pedro, M. A., Zweier, J. L., and Laurindo, F. R. M. (2002) *Free Radic. Biol. Med.* **32,** 446–453
30. Miller, F. J., Jr., Gutterman, D. D., Rios, C. D., Heistad, D. D., and Davidson, B. L. (1998) *Circ. Res.* **82,** 1298–1305
31. Gilbert, H. F. (1998) *Methods Enzymol.* **290,** 26–50
32. Hillson, D. A., Lambert, N., and Freedman, R. B. (1984) *Methods Enzymol.* **107,** 281–294
33. Ushio-Fukai, M., Alexander, R. W., Akers, M., Yin, Q., Fujio, Y., Walsh, K., Griendling, K. K. (1999) *J. Biol. Chem.* **274,** 22699–22704
34. Souza, H. P., Liu, X., Samouilov, A., Kuppusamy, P., Laurindo, F. R. M., and Zweier, J. L. (2002) *Am. J. Physiol.* **282,** H466–H474
35. Yellaturu, C. R., Bhanoori, M., Neeli, I., Rao, G. N. (2002) *J. Biol. Chem.* **277,** 40148–40155
36. Schafer, F. Q., and Buettner, G. R. (2001) *Free Radic. Biol. Med.* **30,** 1191–1212
37. Go, Y.-M., Gipp, J. J., Mulcahy, R. T., and Jones, D. P. (2004) *J. Biol. Chem.* **279,** 5837–5845
38. Xiao, R., Lundstron-Ljung, J., Holmgren, A., and Gilbert, H. (2005) *J. Biol. Chem.* **280,** 21099–21106
39. Doussiere, J., Poinas, A., Blais, C., and Vignais, P. V. (1998) *Eur. J. Biochem.* **251,** 649–658
40. Inanami, O., Johnson, J. L., and Babior, B. M. (1998) *Arch. Biochem. Biophys.* **350,** 36–40
41. Lumb, R. A., and Bulleid, N. J. (2002) *EMBO J.* **21,** 6763–6770
42. Klappa, P., Hawkins, H. C. and Freedman, R. B. (1997) *Eur. J. Biochem.* **248,** 37–42
43. Kimura, T., Imaishi, K., Hagiwara, Y., Horibe, T., Hayano, T., Takahashi, N., Urade, R., Kato, K., and Kikuchi, M. (2005) *Biochem. Biophys. Res. Commun.* **331,** 224–230
44. Kim, J. R., Yoon, H. W., Kwon, K. S., Lee, S. R., and Rhee, S. G. (2000) *Anal. Biochem.* **283,** 214–221
45. Fratelli, M., Demol, H., Puype, M., Casagrande, S., Eberini, I., Salmona, M., Bonetto, V., Mengozzi, M., Duffieux, F., Miclet, E., Bachi, A., Vandekerchkove, J., Gianazza, E., and Ghezzi, P. (2002) *Proc. Natl. Acad. Sci. U. S. A.* **99,** 3505–3510
46. Seshiah, P. N., Weber, D. S., Rocic, P., Valppu, L., Taniyama, Y., and Griendling, K. K. (2002) *Circ. Res.* **91,** 406–413
47. Murphy, J. K., Hoyal, C. R., Livingston, F. R., and Forman H. J. (1995) *Free Radic. Biol. Med.* **18,** 37–45
48. Bardwell, J. C. A., and Beckwith, J. (1993) *Cell* **74,** 769–771
49. Touyz, R. M., Yao, G., and Schiffrin, E. L. (2003) *Arterioscler. Thromb. Vasc. Biol.* **23,** 981–987
50. Li, J.-M., and Shah, A. M. (2003) *J. Biol. Chem.* **278,** 12094–12100
51. Kobayashi, T., Robinson, J. M., and Seguchi, H. (1998) *J. Cell Sci.* **111,** 81–91
52. Catz, S. D., Johnson, J. L., and Babior, B. M. (2002) *Proc. Natl. Acad. Sci. U. S. A.* **99,** 11652–11657
53. Wang, D., Deken, X. D., Milenkovic, M., Song, Y., Pirson, I., Dumont, J. E., and Miot, F. (2005) *J. Biol. Chem.* **280,** 3096–3103